Inorganica Chimica Acta 435 (2015) 66–72

Contents lists available at ScienceDirect

Inorganica Chimica Acta

journal homepage: www.elsevier.com/locate/ica

Study on the synergistic antibacterial effect of silver-carried layered zirconium alkyl-N,N-dimethylenephosphonate

Li Liu, Changhua Liu *, Ling Nie, Ting Jiang, Jing Hong, Xiaomei Zhang, Liehong Luo, Xiaolan Wang

College of Chemistry and Chemical Engineering, Southwest University, Chongqing 400715, PR China

ARTICLE INFO

Article history:
Received 9 April 2015
Received in revised form 4 June 2015
Accepted 5 June 2015
Available online 17 June 2015

Keywords:
Zirconium alkyl-N,N-dimethylenephosphonate
Ag NPs
Synergistic antibacterial

ABSTRACT

A series of zirconium alkyl-N,N-dimethylenephosphonate silver-carrying (Ag-ZRDP) were successfully prepared and their potential applications as synergistic antibacterial materials were investigated. Silver nanoparticles (Ag NPs), of 30 nm in diameter, were tightly anchored onto the zirconium alkyl-N,N-dimethylenephosphonate (ZRDP), increasing the antibacterial activity of the Ag NPs due to a decrease in the extent of nanoparticle aggregation. Due to the synergistic antibacterial effect of the Ag NPs and ZRDP, the Ag-ZRDP showed a better antibacterial activity than Ag NPs and ZRDP with a minimal inhibition concentration (MIC) of 0.25 and 0.25 μg mL^{-1} against *Escherichia coli* and *Staphylococcus aureus*, respectively. Additionally, the Ag-ZRDP did not show obvious cytotoxicity against mammalian cells (A549 cells), even at a concentration of 256 μg mL^{-1}. Collectively, these properties make the newly synthesized Ag-ZRDP potentially superior as disinfectants and antiseptics for various biomedical and biotechnological applications.

1. Introduction

The bacteria in the environment are closely related to human health, which makes it indispensable to perform research into aspects of disinfection to control disease [1]. In the past few decades, considerable effort has been devoted to develop new antibacterial agents capable of fighting bacterial resistance for multiple antibiotics [2–4]. Two main strategies have been implemented to render new antibacterial agents: the first strategy involves synthesizing new antibiotics, which can be costly. In addition, the bacteria can become resistant to them during long-term use. The second strategy involves providing a promising inorganic antibacterial agent that unlike organic antibacterial agents can be utilized in the manufacturing of antibacterial materials and products due to their outstanding properties such as broad-spectrum antibiosis, long-lasting effects, and good heat resistance [5–7]. Silver nanoparticles (Ag NPs) are known to be excellent antibacterial agents with adequate biocompatibility [8] and the ability to permeate bacterial membranes, and inactivate essential respiratory enzymes and proteins responsible for RNA and DNA replication, and thereby inhibit protein function, and more importantly they show limited toxicity to mammalian cells [9]. Nevertheless, Ag NPs are prone to aggregate and form larger clusters owing to their large surface area and high surface energy [10], resulting in poor antibacterial effects. The incorporation of silver into substrates would allow the realization of a distribution system to control silver release while reducing aggregation, and consequently several kinds of silver-carrying antibacterial agents using different inorganic carriers have been investigated, such as activated carbon [11], titanium dioxide [12], water-soluble glass [13], silica wafer [14], poly(acrylic acid) [15,16], graphene oxide [17,18], dopamine [19] and zirconium phosphate [20,21]. However, the antibacterial performance has been found to be time-limited in silver-based materials that kill bacteria via the release of Ag NPs or silver ions [22]. It is well known that zirconium phosphate(α-ZrP)has a layered structure with excellent thermal stability and substantial surface area. The diversification of composite structures can be achieved if phosphinic acid is used as the reactant instead of phosphoric acid during the synthesis of zirconium phosphonate. A series of materials with tailor-made properties can be prepared by an appropriate choice of the organic moiety, for instance, if the organic moiety has coordinative ability, the compound can be used in ion absorption, rare earth coordination, and metal ion coordination catalysis. Organic moieties with strong polar groups or strong non-polar groups will yield compounds that may show hydrophilic or hydrophobic properties. With this being said, to integrate the excellent performance of organic and inorganic antibacterial agents, the organic antibacterial group is introduced into phosphate to obtain organophosphates which have antibacterial and

* Corresponding author.
E-mail address: chliu@swu.edu.cn (C. Liu).

http://dx.doi.org/10.1016/j.ica.2015.06.002
0020-1693/

coordinative activity and can be used as inorganic carriers for Ag NPs. Compounds that can bridge inorganic and organic materials, such as silver carried zirconium alkyl-N,N-dimethylenephosphonate (ZRDP) agents bound to various functional moieties, are available.

Based on above ideas, in this work we have designed and prepared some novel zirconium phosphate derivatives, Zirconium methyl-N,N-dimethylenephosphonate ($Zr[(O_3PCH_2)_2NCH_3]$, ZMDP), zirconium ethyl-N,N-dimethylenephosphonate ($Zr[(O_3PCH_2)_2NC_2H_5]$, ZEDP), zirconium propyl-N,N-dimethylenephosphonate ($Zr[(O_3PCH_2)_2NC_3H_7]$, ZPDP), zirconium n-butyl-N,N-dimethylenephosphonate ($Zr[(O_3PCH_2)_2NC_4H_9]$, ZBDP), zirconium n-hexyl-N,N-dimethylenephosphonate ($Zr[(O_3PCH_2)_2NC_6H_{13}]$, ZHDP), zirconium n-octyl-N,N-dimethylenephosphonate ($Zr[(O_3PCH_2)_2NC_8H_{17}]$, ZODP), possessing the following advantages: (a) n-[bis(phosphonomethyl)amino]-alkyl ($R\text{-}N(CH_2PO_3H_2)_2$, RDP) is a bactericide; (b) synergetic antibacterial activity (when two or more kinds of antibacterial materials are combined together, and the antibacterial properties are better than any single material) can be obtained when mixing n-[bis(phosphonomethyl)amino]-alkyl and Ag NPs; (c) drug resistance of organic bactericide can be resolved during usage; (d) the aggregation of Ag NPs can be inhibited; (e) the problem of free Ag NPs which are cytotoxic to mammalian cells can be solved. The antibacterial activity of Ag-ZRDP was tested against *Escherichia coli* (*E. coli*) and *Staphylococcus aureus* (*S. aureus*). The toxic effect of Ag-ZRDP on A549 cells was determined by using the Cell Counting Kit-8 (CCK-8) assay [23]. The structure and properties of Ag-ZRDP were characterized using a variety of methods: Fourier transform infrared spectroscopy (FTIR), X-ray diffraction (XRD) and transmission electron microscopy (TEM), and scanning electron microscopy (SEM) was utilized to observe the morphology of the bacteria.

2. Experimental

2.1. Materials and methods

All the analytical grade reagents were commercially available and were used without further purification. Methylamine, ethylamine, propylamine, n-butylamine, n-hexylamine and n-octylamine were purchased from Aladdin Company (Shanghai, China). NaCl, D-glucose, $ZrOCl_2{\cdot}8H_2O$, $AgNO_3$ and other reagents were bought from Chengdu Kelong Chemical Reagent Company. Biological reagent Muellor Hinton agar, peptone, beef extract was provided by Beijing Aoboxing Bio-Tech Co., Ltd. Deionized water was used for preparation of all solutions. All ^1H and ^{31}P NMR measurements were recorded on a Bruker AVANCE III 600 MHz spectrometer using TMS as an internal standard for a D_2O solution and reported in parts per million (ppm). The Fourier Transform infrared (FT-IR) spectra of the nanocomposites were recorded in KBr discs using a Nicolet (Madison, WI, USA) 170SX FTIR spectrometer in the range of 4000–600 cm^{-1}, in the attenuated total reflection mode. X-ray diffraction was performed on a XRD-3D, Puxi, (Beijing, China) X-ray diffractometer under the following conditions: Nickel filtered Cu Kα radiation (λ = 0.15406 nm) at a current of 20 mA and a voltage of 36 kV. The scanning rate was 4° min^{-1} in the angular range of 3–40° (2θ). The concentration of silver ions was measured by ICP single channel scanning spectrometer, Puxi, (Beijing, China) TPS-7000. The specific surface area was measured by Quantachrome Instruments (USA) QUA211007. The micromorphologies of all the samples were investigated by transmission electron microscope (TEM) using a JEM-2010 (Japan) at an accelerating voltage of 200 kV. The surface morphologies of bacteria of the control and treated with Ag-ZRDP were observed by scanning electron microscope (SEM) using a HITACHI S-4800, Japan. All the samples were placed on round brass stubs and sputter coated with gold and then scanned at an accelerating voltage of 20 kV.

2.2. Synthesis of Ag NPs

In a typical process [24], Ag NPs were synthesized via ascorbic acid reduction of silver nitrate using ethanol as a solvent in the presence of poly (N-vinyl-2-pyrrolidone) (PVP). $AgNO_3$ (0.2 g) and PVP (0.5 g) were dissolved in 40 mL ethanol, and then added drop wise 10 mL of ethanol solution containing 0.1 mol L^{-1} L-ascorbic acid with vigorous stirring at room temperature, resulting in a colloidal solution of silver nanoparticles.

2.3. Preparation of RDP, ZRDP and Ag-ZRDP

2.3.1. RDP

n-[Bis(phosphonomethyl)amino]-alkyl ($R\text{-}N(CH_2PO_3H_2)_2$, RDP) was synthesized by the Mannich-type reaction according to literature [25]. H_3PO_3 (0.2 mol) and alkylammonium (0.1 mol) were mixed in a 250 mL three-necked flask then concentrated HCl aqueous solution (10 mL) was slowly added with stirring. Then, the temperature of mixture was brought to 110 °C followed by adding drop wise a 100% excess of 37% aqueous formaldehyde solution (15 mL) during 1–2 h and refluxing for another 2–3 h. Subsequently, the mixture was stored at room temperature overnight with stirring, resulting in a crystallized product. The NMR of RDP was presented in the Supporting information (S1).

2.3.2. ZRDP

A solution of RDP (0.01 mol) in 100 mL water was added into $ZrOCl_2{\cdot}8H_2O$ (3.23 g, 0.01 mol) in 100 mL water with vigorous stirring at 60–70 °C for 6 h. Subsequently, the mixture was filtered and washed with deionized water until the pH of solution was near 5–6. Dry ZRDP was obtained at 60 °C for 48 h under vacuum. The chemical equations for the synthesis of ZRDP are shown in Scheme 1.

2.3.3. Ag-ZRDP

ZRDP was dispersed in deionized water to obtain a suspension of 10.0 mass% and transferred to a 1 L reaction kettle followed by adding different amounts of $AgNO_3$ (final concentration from 0.05 to 1.6 mass%) with stirring. Then, the temperature was maintained at 60 °C for 3 h. Subsequently, the mixture was filtered and washed with deionized water resulting in the Ag-ZRDP sample. The sample was obtained at 45 °C for 12 h under vacuum.

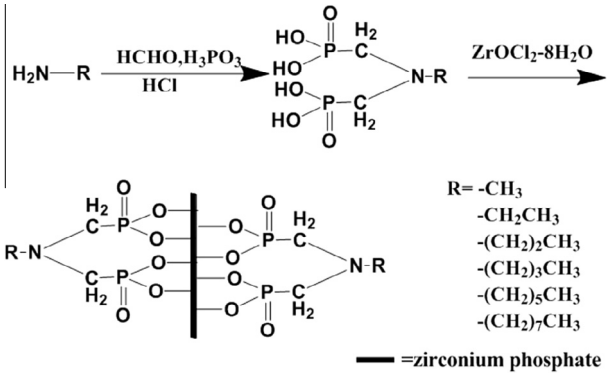

Scheme 1. The chemical equations for the synthesis of ZRDP.

2.4. Antibacterial tests

2.4.1. Antibacterial assays

The minimal inhibitory concentration (MIC, μg mL^{-1}) was measured by means of standard two-fold serial dilution method in 96-well microtest plates according to the National Committee for Clinical Laboratory Standards (NCCLS) [26,27]. The tested microorganism strains were provided by the School of Pharmaceutical Sciences, Southwest University. The growth of bacteria was visually and spectrophotometrically monitored and the experiments were performed thrice times. The Ag NPs, ZRDP, and Ag-ZRDP were evaluated for their antibacterial activities against Gram-positive bacteria (*S. aureus ATCC25923*) and Gram-negative bacteria (*E. coli JM109*). The bacterial suspension was adjusted with sterile saline to a concentration of 3×10^5 cfu mL^{-1}. Stock solutions were suspended in beef broth to a concentration of 1024 μg mL^{-1}, then a two-fold dilution series of 100 μL quantitative samples solutions in Luria broth (LB) were made on 96-well microplates and kept in an incubator for 24 h at 37 °C. The MIC was read by the visual turbidity of the tubes noted both before and after incubation.

2.4.2. Bactericidal kinetics testing

Ag-ZPDP was added to tubes containing the tested bacteria at a concentration of 3×10^5 cfu mL^{-1} in Luria broth (LB) medium and the tubes were kept in an incubated shaker at 37 °C. The initial addition time of the *E. coli* and *S. aureus* broth to the tubes was established as time zero and 50 μL aliquots were withdrawn from each of the tubes at set time intervals and plated on LB agar plates. The plates were incubated at 37 °C for 48 h and then the bacterial colonies were counted in order to calculate the antibacterial activity.

2.4.3. Preparation of SEM samples

Ag-ZPDP was added into the bacterial suspension (10 mL, *S. aureus ATCC25923* and *E. coli JM109*) of 3×10^5 cfu mL^{-1} in sterile test tubes. The test tubes were then shaken at 37 °C for 1 h followed by centrifugation and three consecutive washings with sterile PBS (pH 7.2). The bacteria were then fixed by 4% glutaraldehyde for 4 h followed by step dehydration using 20%, 50% and 80% v/v water/ethanol mixture and lastly ethanol absolute. The micromorphologies of all the samples were investigated by SEM after sputtering a thin gold layer.

2.5. Cytotoxicity assay of Ag-ZRDP

2.5.1. Cell culture

A549 cells were cultured and maintained in DMEM (GIBCO, USA), supplemented with 10% fetal bovine serum (FBS) (GIBCO, USA), 100 U mL^{-1} penicillin G, and 100 μg mL^{-1} streptomycin sulfate. Cells were maintained at 37 °C in 5% CO_2 in a humidified atmosphere.

2.5.2. Vitro cytotoxicity of Ag-ZRDP

The toxic effect of Ag-ZRDP on A549 cells was determined by using the Cell Counting Kit-8 (CCK-8) assay based on 2-(2-methoxy-4-nitro phenyl)-3-(4-nitrophenyl)-5-(2,4-disulfophenyl)-2H-tetrazolium (WST-8) [28]. The Ag-ZRDP solution was diluted with F-12, which contained 10% FBS (2-fold serial dilution). A549 cells were cultured in 96-well plates at a density of 2×10^4 cells per well which grew to 80% confluence in the presence of 100 μL of F-12 with 10% FBS, followed by three washings with phosphate-buffered saline (PBS), and added to 100 μL of F-12 with Ag-ZRDP at a concentration of 0, 8, 16, 32, 64, 128 and 256 μg mL^{-1}, and incubated for 48 or 72 h. Cellular viability was detected on OD450 nm.

3. Results and discussion

3.1. Structural and morphological studies

3.1.1. FTIR spectral analysis

The FTIR spectra of ZPDP and Ag-ZRDP are shown in Fig. 1. In both of the FTIR spectra, a characteristic strong peak at 3471 cm^{-1} was observed that is attributed to the O—H stretching. Peaks at 1457 and 1379 cm^{-1} were assigned to bending of the CH_3 group and the peaks at 1162 and 1015 cm^{-1} represent the P═O vibrations [29]. With an increase in the alkyl chain length, peaks appearing at 2952 and 2855 cm^{-1} increase in intensity, which can be assigned to the stretching vibration of the CH_2 group [30]. There is no difference between the FTIR spectra of ZRDP and Ag-ZRDP, inferred that Ag NPs are loaded onto the ZRDP by physical adsorption, and they will not cause the change of infrared spectrum peak.

3.1.2. XRD pattern analysis

The XRD patterns of ZPDP and Ag-ZRDP provided an insight into the crystal-phase composition of the products, as shown in Fig. 2. Compared with the XRD spectra of ZPDP, it is observed that the crystal structure of the carrier was not obviously affected by the loading of Ag NPs. However, a sharp and intensive diffraction peak at 38.3° appeared, which matched well with the (1 1 1) planes of the Ag NPs [31] and indicates a highly organized Ag NPs crystal structure. An inconspicuous diffraction peak at approximately 5° can be observed and with an increase of the alkyl chain length, the diffraction peak shifts to a lower diffraction angle based on the Bragg formula (Eq. (1), as follows:

$$2 * d * \sin\theta = n * \lambda \quad (1)$$

The increase of the samples' layer spacing has gradually taken place, these results are summarized in Table 1.

3.1.3. TEM measurements

The morphology of ZEDP, Ag-ZEDP, ZBDP, Ag-ZBDP, ZHDP, Ag-ZHDP, ZODP and Ag-ZODP were investigated by TEM, as shown in Fig. 3. Compared with the TEM of ZRDP, the TEM of Ag-ZRDP has Ag NPs particles exist. Results indicate that the Ag NPs produced by self-reduction show a homogeneous distribution and impregnated in the ZRDP layers, possessing diameters ranging from 18 to 42 nm and an average particle size of 30 nm. The above analysis suggests that Ag NPs were successfully formed and

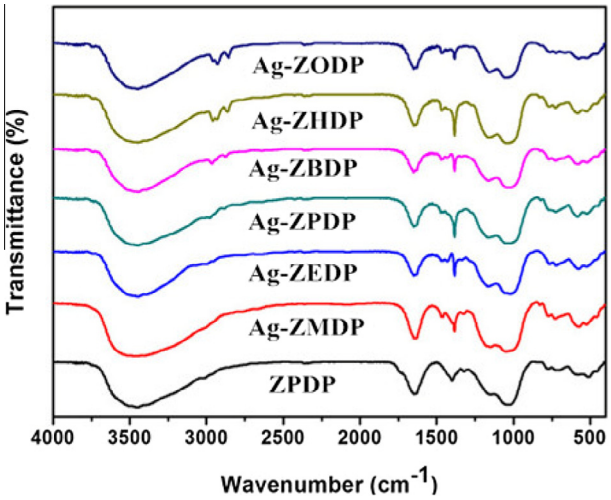

Fig. 1. FTIR spectrum of ZPDP, Ag-ZRDP.

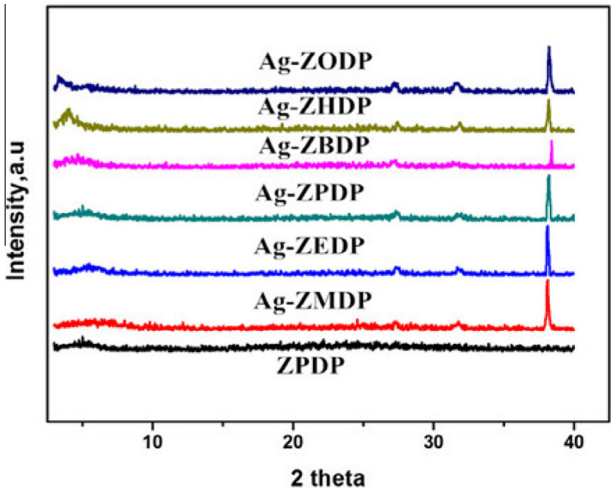

Fig. 2. XRD patterns of ZPDP and Ag-ZRDP powders.

Table 1
The interlayer distance of Ag-ZRDP.

Sample	2θ (°)	d_0 (nm)
Ag-ZMDP	5.938	1.487
Ag-ZMDP	5.467	1.615
Ag-ZPDP	4.976	1.774
Ag-ZBDP	4.688	1.883
Ag-ZHDP	4.014	2.200
Ag-ZODP	3.341	2.642

Table 2
Antibacterial activities of $ZrOCl_2$, Ag NPs, RDP, ZRDPA, Ag-ZRDP (Ag NPs, 0.4%) and the contrast materials.

Sample	MIC ($\mu g\ mL^{-1}$)		Comments
	S. aureus (ATCC25923)	*E. coli* (JM109)	
$ZrOCl_2$	8×10^3	8×10^3	
MDP	4×10^3	6.4×10^3	
EDP	3.2×10^3	4×10^3	
PDP	2×10^3	2×10^3	
BDP	1.6×10^3	2×10^3	
HDP	–	–	
ODP	–	–	
Ag NPs	64	128	
ZMDP	56[a]	64	
ZEDP	36[a]	53[a]	
ZPDP	30[a]	32	
ZBDP	28[a]	28[a]	
ZHDP	28[a]	26[a]	
ZODP	16	20[a]	
Ag-ZMDP	5[a]	6[a]	
Ag-ZEDP	3[a]	4	
Ag-ZPDP	0.75[a]	1	
Ag-ZBDP	0.75[a]	0.75[a]	
Ag-ZHDP	0.5	0.75[a]	
Ag-ZODP	0.25	0.25	
Ag-TiO_2		50	Ref. [35]
Ag-GO		50	Ref. [36]
Ag-SiO_2		10	Ref. [37]
Oxacillin	0.4		Ref. [38]
AgZrP		100	Ref. [20]

To further determine the more specific MIC of Ag-ZRDP, in a certain range of concentration (based on twofold dilution method), different concentrations of Ag-ZRDP were prepared, those data are marked with a. Because HDP and ODP neither dissolve nor dispersed in water, their antibacterial activity cannot be investigated.

homogeneously dispersed in the ZRDP, which agrees well with the XRD data obtained.

3.2. Antibacterial activity

3.2.1. Minimum inhibitory concentration testing

MIC is defined as the lowest concentration ($\mu g\ mL^{-1}$) at which a compound will kill more than 99% of the added bacteria. A lower MIC corresponds to a higher antibacterial effectiveness. The obtained results for Ag NPs, ZRDP and Ag-ZRDP against *E. coli* and *S. aureus* are displayed in Table 2. The *in vitro* antibacterial evaluation demonstrated that the Ag NPs, ZRDP and Ag-ZRDP effectively inhibited the growth of the tested microorganisms and potent antibacterial activity. Compared to the results reported in the literature [11–14], it was found that the carriers (ZRDP) possessed self-antibacterial activity, which has not been observed before. It was also observed that when the alkyl chain increased, the antibacterial activity was enhanced; this result is consistent with results reported in the literature [32,33], and has been attributed to the fact that the main composition of the bacterial cell is hydrophobic and when the length of the alkyl chain increases, its hydrophobicity also increases (see to S2), causing an enhancement

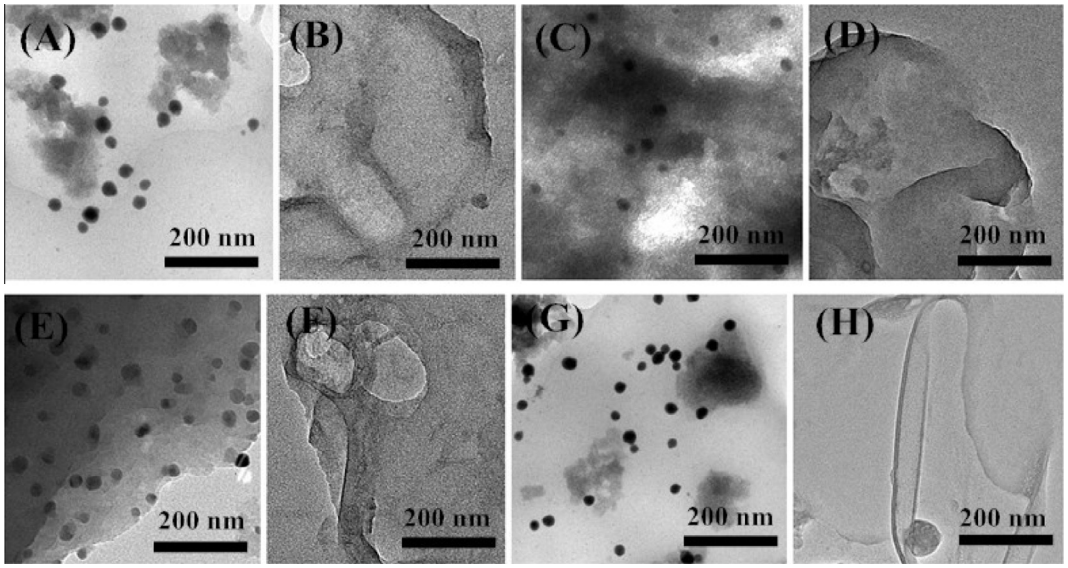

Fig. 3. TEM image of Ag-ZEDP (A), ZEDP (B), Ag-ZBDP (C), ZBDP (D), Ag-ZHDP (E), ZHDP (F), Ag-ZODP (G), ZODP (H).

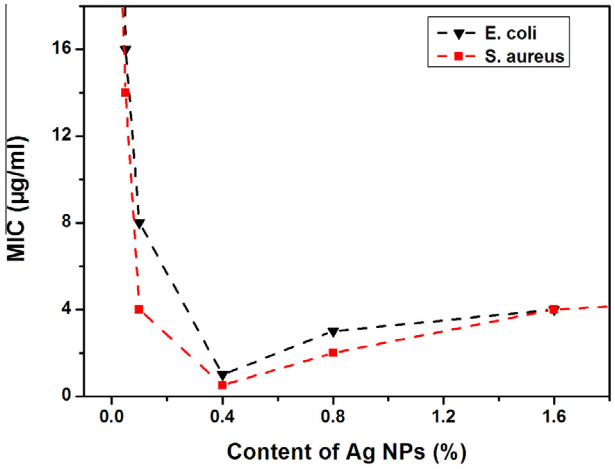

Fig. 4. Different Ag NPs contenting of Ag-ZPDP.

of bacteria adsorption. When the layer spacing of the samples increased, the release of silver ion from the interlayer was more readily. At the same time, results showed that the Ag-ZRDP exhibited a synergetic antibacterial activity against the two organisms between that of the ZRDP and the Ag NPs. It can be observed in Fig. 4 that the optimized Ag NPs content was 0.4 wt.% with an MIC of 0.75 μg mL^{-1} against *S. aureus* and 1 μg mL^{-1} against *E. coli*. This is attributed to the fact that the content of Ag NPs is directly proportional to the synergetic antibacterial activity of the samples in a certain range of Ag NPs concentration. When the specific surface area (Table 3) of the material was reduced, the adsorption ability of the bacteria and the release of silver ion decreased; thus, reducing the antibacterial activity of the final sample, which was an important factor when the concentration of Ag NPs is over 0.4 wt.%. Moreover, all materials demonstrated higher antibacterial activity against *S. aureus* than against *E. coli*, primarily attributed to the structure of the bacterial membrane. All Gram-negative bacteria possess an outer membrane due to the presence of lipopolysaccharide (LPS) molecules [34], which provides the bacterium with a hydrophilic surface. The lipid components and the inner core of the LPS molecules contain anionic groups (phosphate, carboxyl), which contribute to the stability of the LPS layer. The structure of *S. aureus* is rough so that it is susceptible for small antibacterial molecular agents to diffuse into the organism. Gram-negative *E. coli* has a more complicated cell wall and a layer similar to a sieve, making it arduous for antibacterial agents to cross the capsule. Results indicate that the antibacterial effects of the Ag-ZRDP was better than that of the silver-carried TiO_2 [35], graphene oxide [36], SiO_2 [37], and oxacillin [38]. In this work, the MIC of the optimized Ag-ZODP achieved 0.25 μg mL^{-1} against *S. aureus* and *E. coli*. Tan et al. reported that the MIC of silver-carried zirconium phosphate was 100 μg mL^{-1} against *E. coli* [20]. In this work, it was found that the antibacterial effect of n-[bis(methyl)amino]-alkyl decorated zirconium phosphate has been drastically improved. Results proved that ZRDP is more suitable than zirconium phosphate as carriers of antibacterial materials, which may contribute to a synergetic antibacterial activity between the antibacterial organic functional groups and the inorganic Ag NPs on the Ag-ZRDP.

Table 3
The specific surface area of Ag-ZPDP.

Content (%)	Specific surface area (m^2 g^{-1})
0.4	9.269
0.8	9.165
1.6	8.348

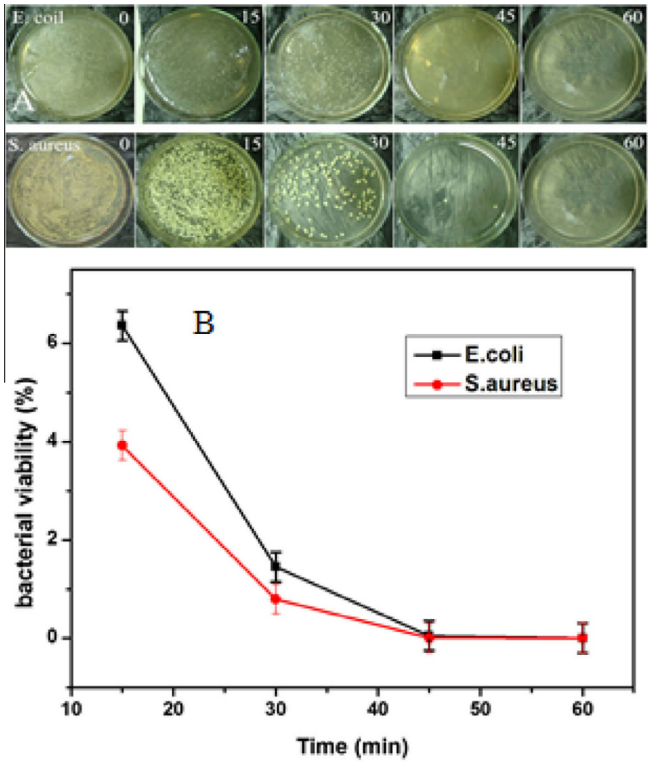

Fig. 5. (A) Representative photographs of the bactericidal activity of Ag-ZPDP against Gram-negative *E. coli* and Gram-positive *S. aureus*: From left-hand side to right-hand side: 0, 15, 30, 45, and 60 min, respectively (the addition time of Ag-ZPDP). The concentration of Ag-ZPDP was 1 and 0.75 μg mL^{-1} toward *E. coli* and *S. aureus*, respectively. (B) The bacterial viability after treated with Ag-ZPDP for various quantities of time.

3.2.2. Bactericidal kinetics assay

To further determine the antibacterial activity of Ag-ZRDP, the kinetics of Ag-ZPDP toward Gram-negative *E. coli* and Gram-positive *S. aureus* were investigated. A 10 mL Ag-ZPDP solution (1 and 0.75 μg mL^{-1} toward *E. coli* and *S. aureus*, respectively) containing approximately 3×10^5 cfu mL^{-1} of *E. coli* or *S. aureus* in LB broth was added to tubes, which were kept in an incubated shaker at 37 °C. Aliquots from each suspension were withdrawn at set time intervals, plated on LB agar plates, and incubated for 48 h. Fig. 5 illustrates pictures of the bactericidal activity of Ag-ZPDP toward *E. coli* and *S. aureus*. Colonies formed after incubation and were counted as shown in Fig. 5A, corresponding to the number of live bacteria in each suspension at the time of the aliquot withdrawal. The bacterial viability was calculated using Eq. (2) as follows:

$$\text{Bacterial viability}\,(\%) = \frac{N_t}{N_0} \times 100\% \qquad (2)$$

where N_0 and N_t correspond to the number of colonies calculated at time zero and set time intervals, respectively. Fig. 5 (from left to

Table 4
The number of colonies (corresponded to the number of live bacteria) treated with Ag-ZPDP for different time.

Time (min)	*E. coli*	*S. aureus*
0	$15\,000^a$	$15\,000^a$
15	954^b	588^b
30	218^b	132^b
45	8^b	2^b
60	0^b	0^b

The numbers are marked with a come from theoretical calculation, and the numbers are marked with b come from experimental result.

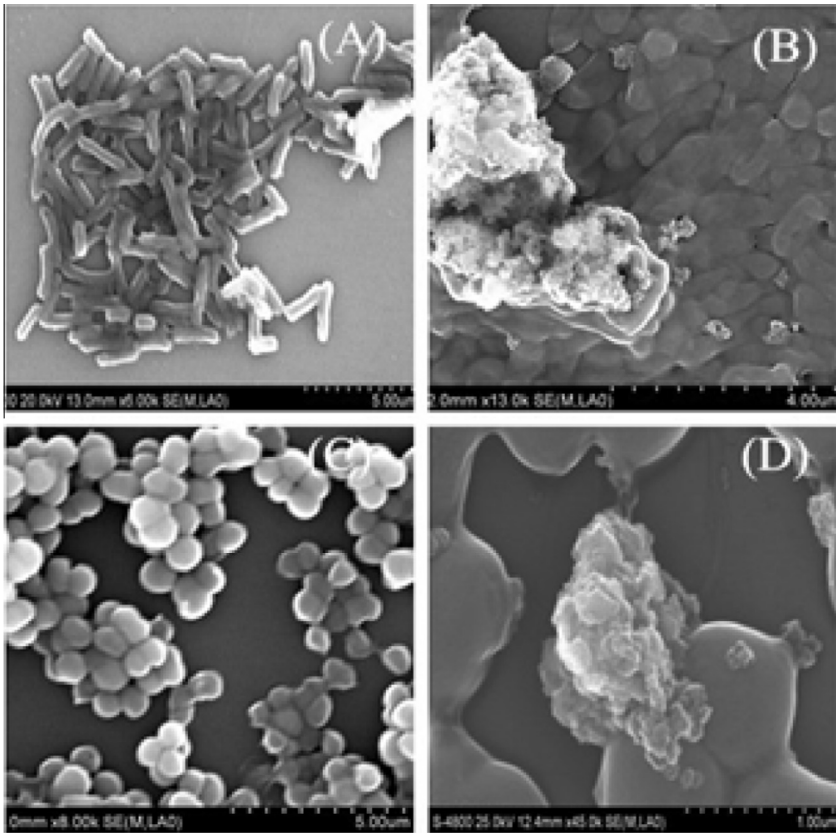

Fig. 6. SEM images of *E. coli* (A) untreated and (B) treated; *S. aureus* (C) untreated and (D) treated with Ag-ZRDP (1 and 0.75 μg mL^{-1} toward *E. coli* and *S. aureus*, respectively) for 1 h.

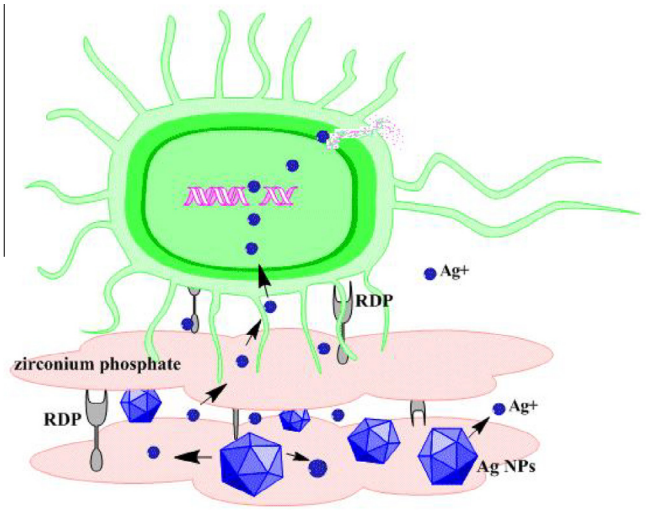

Fig. 7. Schematic illustration of the possible antibacterial mechanism of Ag-ZRDP.

right) shows different addition times of the Ag-ZPDP samples of 0, 15, 30, 45, and 60 min, respectively, in which the results are summarized in Table 4. It can be seen in Fig. 5A that after 60 min of incubation, a negligible amount of *E. coli* and *S. aureus* colonies were found. Fig. 5B suggests that only 6.36% and 3.92% live *E. coli* and *S. aureus* were detected after 15 min. Compared with the literature, the antibacterial activity kinetics for Ag-ZPDP was improved compared to results reported by Agnihotri et al., which needed 120 and 90 min to achieve ⩾99.9% *E. coli* and *S. aureus* reduction, respectively [39].

3.2.3. SEM measurements

To obtain visual insight into the antibacterial action of Ag-ZRDP, SEM studies were performed. SEM images of both *E. coli* and *S. aureus* treated with Ag-ZPDP (1 and 0.75 μg mL^{-1} toward *E. coli* and *S. aureus*, respectively) for 1 h and additional control groups were acquired (Fig. 6). All the control groups demonstrated the presence of normal cells (Fig. 6A and C for *E. coli* and *S. aureus*, respectively) with preserved cell membranes. However, irregularly shaped and essentially dead bacteria were observed upon treatment with Ag-ZPDP (Fig. 6B and D for *E. coli* and *S. aureus*, respectively). The

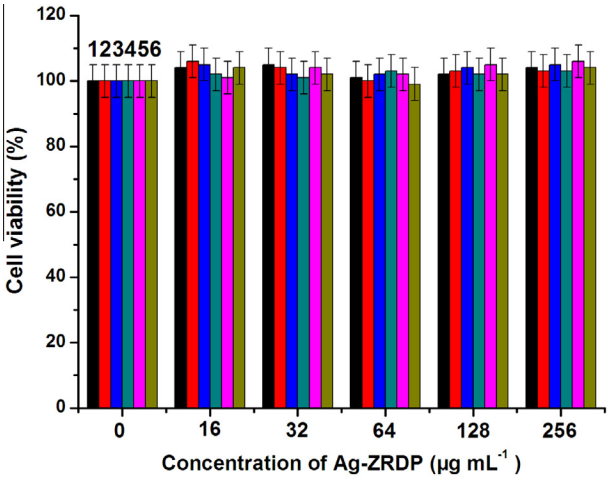

Fig. 8. Cytotoxicity assay of Ag-ZRDP on A549 cells tested by CCK-8 Kit. Corresponding sample of each number: 1, Ag-ZMDP; 2, Ag-ZEDP; 3, Ag-ZPDP; 4, Ag-ZBDP; 5, Ag-ZHDP; 6, Ag-ZODP.

antibacterial mechanism (Fig. 7) proves to be as follows: ZRDP, which have an identical structure to that of montmorillonites [40] and can form zwitterion structures by transporting H^+ to N atoms, utilizes its large specific surface area to absorb the bacteria from the solution and immobilize them with the assistance of its excellent adsorption capacity. The cations of ZRDP will also interact with the bacterial cell membrane, making holes, and disrupting the cell membrane, which may lead to the loss of cytoplasmic constituents and ultimately cell death. Silver in its metallic state can react with moisture to be ionized, releasing highly reactive Ag^+ ions, in which the ionized silver can bind to proteins causing structural changes in the cell wall and also in the nuclear membranes provoking cell death [41].

Ag^+ also forms complexes with bases contained in the DNA and RNA that inhibit the microorganism replication [42]. In conclusion, the synergetic antibacterial function between ZRDP and Ag NPs may lead to the loss of cytoplasmic constituents and eventually cell death.

3.3. Cytotoxicity assay on mammalian cells

A good antibacterial agent needs to be nontoxic to humans and animals. In order to prepare Ag-ZRDP for *in vivo* trials, primary human cells (A549 cells) are used to test their cytotoxicity using a commercial kit (CCK-8Kit) that produces soluble purple formazan in the presence of viable cells and its absorbance increases linearly as cells proliferate. Kawata et al. reported that the viability of human cells incubated with free Ag NPs (3 $\mu g\ mL^{-1}$) for 24 h distinctly decreased to 50% [23]. In this work, results (Fig. 8) demonstrate that Ag-ZRDP did not affect the viability of A549 cells even at a concentration of 256 $\mu g\ mL^{-1}$ (containing 4.1 $\mu g\ mL^{-1}$ Ag NPs), which makes them non-cytotoxic to mammalian cells. The explanation of this contradictory results may be due to the behavior of Ag NPs tightly immobilized on the zirconium phosphate interlayer and free Ag NPs are not allowed to be released to enter into cells and induce cytotoxicity.

4. Conclusions

In the present study, a facile method to prepare silver-carried layered zirconium alkyl-N,N-dimethylenephosphonate was successfully demonstrated. Due to the synergistic antibacterial effect of Ag NPs and ZRDP, Ag-ZRDP behaved with an enhanced antibacterial activity relative to the single counterparts of Ag NPs and ZRDP. When the Ag NPs content was 0.4 wt.%, the minimal inhibition concentrations (MIC) of Ag-ZODP was 0.25 and 0.25 $\mu g\ mL^{-1}$ against *E. coli* and *S. aureus*, respectively. The CCK-8 assay illustrated that there is no cytotoxicity to A549 cells at a concentration of 256 $\mu g\ mL^{-1}$. The non-toxic properties of Ag-ZRDP to primary human cells may facilitate its clinical application.

Appendix A. Supplementary material

Supplementary data associated with this article can be found, in the online version, at http://dx.doi.org/10.1016/j.ica.2015.06.002.

References

[1] A. Blanazs, R. Verber, O.O. Mykhaylyk, A.J. Ryan, J.Z. Heath, C.I. Douglas, S.P. Armes, J. Am. Chem. Soc. 134 (2012) 9741.
[2] I. Aissa, M. Bouaziz, F. Frikha, R.B. Mansour, Y. Gargouri, Process Biochem. 47 (2012) 2356.
[3] Z.G. Chen, Q. Zhu, M.H. Zong, Z.X. Gu, Y.B. Han, Process Biochem. 46 (2011) 1649.
[4] D. Campoccia, L. Montanaro, P. Speziale, C.R. Arciola, Biomaterials 31 (2010) 6363.
[5] B. Jia, Y. Mei, L. Cheng, J. Zhou, L. Zhang, ACS Appl. Mater. Interfaces 4 (2012) 2897.
[6] S. Qian, Y. Qiao, X. Liu, J. Mater. Chem. B 2 (2014) 7475.
[7] Y.S. Ko, Y.H. Joe, M. Seo, K. Lim, J. Hwang, K. Woo, J. Mater. Chem. B 2 (2014) 6714.
[8] D. Li, Z. Liu, Y. Yuan, Y. Liu, F. Niu, Process Biochem. 50 (2015) 357.
[9] D.M. Eby, N.M. Schaeublin, K.E. Farrington, S.M. Hussain, G.R. Johnson, ACS Nano 3 (2009) 984.
[10] S.J. Yu, Y.G. Yin, J.F. Liu, Environ. Sci. Processes Impacts 15 (2013) 78.
[11] S. Zhang, R. Fu, D. Wu, W. Xu, Q. Ye, Z. Chen, Carbon 42 (2004) 3209.
[12] L.Z. Zhang, J.C. Yu, H.Y. Yip, Q. Li, K.W. Kwong, A.W. Xu, P.K. Wong, Langmuir 19 (2003) 10372.
[13] E. Vernè, S.D. Nunzio, M. Bosetti, P. Appendino, C.V. Brovarone, G. Maina, M. Cannas, Biomaterials 26 (2005) 5111.
[14] Y. Zhou, X. Jiang, J. Tang, Y. Su, F. Peng, Y. Lu, Y. He, J. Mater. Chem. B 2 (2014) 691.
[15] Y. Tao, Y. Lin, Z. Huang, J. Ren, X. Qu, Talanta 88 (2012) 290.
[16] Z. Huang, Y. Tao, F. Pu, J. Ren, X. Qu, Chem. Eur. J. 18 (2012) 6663.
[17] X. Ran, H. Sun, F. Pu, J. Ren, X. Qu, Chem. Commun. 49 (2013) 1079.
[18] Y. Tao, Y. Lin, Z. Huang, J. Ren, X. Qu, Analyst 137 (2012) 2588.
[19] Y. Lin, C. Chen, C. Wang, F. Pu, J. Ren, X. Qu, Chem. Commun. 47 (2011) 1181.
[20] S. Tan, Y. Ouyang, L. Zhang, Y. Chen, Y. Liu, Mater. Lett. 62 (2008) 2122.
[21] M. Nishioka, T. Nishimura, A. Ookubo, M. Taya, Biotechnol. Lett. 25 (2003) 1263.
[22] H. Kong, J. Jang, Langmuir 24 (2008) 2051.
[23] K. Kawata, M. Osawa, S. Okabe, Environ. Sci. Technol. 43 (2009) 6046.
[24] Y. Sun, B. Wiley, Z.Y. Li, Y. Xia, J. Am. Chem. Soc. 126 (2004) 9399.
[25] K. Moedritzer, R.R. Irani, J. Org. Chem. 31 (1966) 1603.
[26] N. Özbek, H. Katırcıoğlu, N. Karacan, T. Baykal, Bioorg. Med. Chem. 15 (2007) 5105.
[27] A.A. Kadi, N.R. El-Brollosy, O.A. Al-Deeb, E.E. Habib, T.M. Ibrahim, A.A. El-Emam, Eur. J. Med. Chem. 42 (2007) 235.
[28] H. Tominaga, M. Ishiyama, F. Ohseto, K. Sasamoto, T. Hamamoto, K. Suzuki, M. Watanabe, Anal. Commun. 36 (1999) 47.
[29] A.V. Raghu, G.S. Gadaginamath, H.M. Jeong, N.T. Mathew, S.B. Halligudi, J. Appl. Polym. Sci. 113 (2009) 2747.
[30] K. Gholivand, F. Ghaziani, R. Yaghoubi, Z. Hosseini, Z. Shariatinia, J. Enzyme Inhib. Med. Chem. 25 (2010) 827.
[31] T.T. Baby, S. Ramaprabhu, J. Mater. Chem. 21 (2011) 9702.
[32] N. Joondan, P. Caumul, M. Akerman, S. Jhaumeer-Laulloo, Bioorg. Chem. 58 (2015) 117.
[33] N. Joondan, S. Jhaumeer-Laulloo, P. Caumul, Microbiol. Res. 169 (2014) 675.
[34] H. Nikaido, J. Bacteriol. 178 (1966) 5853.
[35] N. Perkas, A. Lipovsky, G. Amirian, Y. Nitzan, A. Gedanken, J. Mater. Chem. B 1 (2013) 5309.
[36] J. Ma, J. Zhang, Z. Xiong, Y. Yong, X.S. Zhao, J. Mater. Chem. 21 (2011) 3350.
[37] S.K. Rastogi, V.J. Rutledge, C. Gibson, D.A. Newcombe, J.R. Branen, A.L. Branen, Biol. Med. 7 (2011) 305.
[38] G. Belofsky, M. Aronica, E. Foss, J. Diamond, F. Santana, J. Darley, D. Ferreira, J. Nat. Prod. 77 (2014) 1140.
[39] S. Agnihotri, S. Mukherji, S. Mukherji, RSC Adv. 4 (2014) 3974–3983.
[40] S.L. Lemke, P.G. Grant, T.D. Phillips, J. Agric. Food Chem. 46 (1988) 3789.
[41] A. Muñoz-Bonilla, M. Fernández-García, Prog. Polym. Sci. 37 (2012) 281.
[42] M. Rai, A. Yadav, A. Gade, Biotechnol. Adv. 27 (2009) 76.